一般社団法人 電子情報通信学会
THE INSTITUTE OF ELECTRONICS,
INFORMATION AND COMMUNICATION ENGINEERS

信学技報
IEICE Technical Report

Orthogonal Code-Multiplexed Frequency-Domain Single-Carrier Spread Spectrum

Amnart BOONKAJAY † and Fumiyuki ADACHI ‡

† ‡ Department of Communications Engineering, Graduate School of Engineering, Tohoku University
6-6-05 Aza-Aoba, Aramaki, Aoba-ku, Sendai, Miyagi, 980-8579 Japan
E-mail: †amnart@mobile.ecei.tohoku.ac.jp ‡adachi@ecei.tohoku.ac.jp

Abstract The authors have proposed a frequency-domain single-carrier spread spectrum (SC-FDSS) transmission technique, which achieves better bit-error rate (BER) and better power amplifier-dependent energy efficiency comparing with time-domain spread spectrum (TDSS). However, its wider transmission bandwidth leads to low spectrum efficiency, implying that a multiplexing technique is necessary. In this paper, we introduce an orthogonal code multiplexing technique for the FDSS called multi-code single-carrier FDSS (MC-SC-FDSS) for code division multi-access. The signal block to be transmitted is firstly transformed into frequency-domain signal by discrete Fourier transform (DFT), and then code multiplexing is done to achieve narrower transmit bandwidth. Joint frequency-domain equalization based on minimum mean-square error criterion (MMSE-FDE) and de-spreading is carried out for acquiring frequency diversity gain. Theoretical analysis and simulation results in terms of BER and PAPR of both single-code and multi-code SC-FDSS are shown and compared with conventional TDSS and multi-carrier SS (MCSS)

Keyword Single-carrier (SC) transmission, spread spectrum (SS), code-division multiplexing (CDM)

1. Introduction

Broadband wireless channel is characterized as a frequency-selective fading channel, in which inter-symbol interference (ISI) degrades system performance in terms of bit-error rate (BER) [1]. Orthogonal frequency division multiplexing (OFDM) is robust against fading but its high peak-to-average power ratio (PAPR) of transmit signal is the main drawback [2]. On the other hand, single-carrier (SC) transmission [3] is more attractive for uplink communication in LTE-Advanced (LTE-A) system because of lower PAPR compared to OFDM, while the use of frequency-domain equalization (FDE) can effectively suppress the impact of ISI [4].

SC signal can be alternatively generated by inserting discrete Fourier transform (DFT) into conventional OFDM transmitter [5]. By using this approach, frequency-domain signal processing, where transmit/receive filtering can be simply employed as one-tap multiplication [6], is approachable. Flexibility of signal manipulation, e.g. mapping, is also able to be implemented.

The authors have recently proposed a transmission approach taking advantage of the use of frequency-domain processing called SC with frequency-domain spread spectrum (SC-FDSS) [7], spreading and de-spreading are all done in frequency domain by simple copying/mapping and combining frequency components, respectively. Performance of SC-FDSS has been evaluated in various aspects [7-9], and found that SC-FDSS provides better BER performance compared to SC time-domain spread spectrum (SC-TDSS) as a contribution of additional frequency diversity gain. PAPR of SC-FDSS waveform is higher than SC-TDSS when spreading factor (*SF*) increases, but still less than multi-carrier (MC) waveform. Power amplifier-dependent energy efficiency (EE) [10] of both transmission schemes have been evaluated in [9] and found that SC-FDSS achieves better EE due to its time-domain interleaving property, even though its PAPR is higher than SC-TDSS. However, similar to other spread spectrum transmission techniques, multiplexing technique is indispensable in order to improve the spectrum efficiency.

In this paper, we introduce a multi-code SC-FDSS (MC-SC-FDSS). Orthogonal code multiplexing and simple frequency mapping are applied in frequency domain. At the receiver, joint FDE based on minimum mean-square error (MMSE-FDE) and de-spreading is employed for acquiring frequency diversity gain. Theoretical analysis and simulation results of the proposed transmission scheme, both single-code and multi-code transmissions, are shown in terms of BER, and compared to conventional TDSS [11] and multi-carrier SS (MCSS) [12]. PAPR is also important to be discussed because it is directly related to energy efficiency.

The rest of this paper is organized as follows. System models of single-code and multi-code SC-FDSS are described in Section 2. Section 3 provides theoretical analysis on signal-to-interference plus noise power ratio (SINR) and conditional BER. Section 4 shows the performance evaluation, and Section 5 concludes the paper.

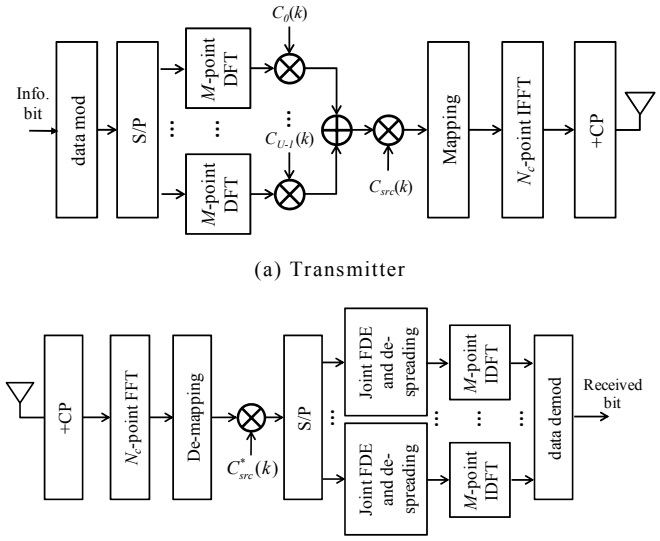

(a) Transmitter

(b) Receiver

Fig.1 Transmission system models.

2. Transmission System Models

Fig. 1 shows single-user baseband transmission system models of (a) transmitter and (b) receiver of MC-SC-FDSS, respectively. In multi-code transmission, transmit data symbol sequence is serial-to-parallel converted into U parallel sequences, where each parallel sequence consists of M modulated symbols. Each parallel sequence is transformed into frequency-domain signal, followed by orthogonal spreading (spreading factor is SF) and U code-multiplexing, implying that equivalent spreading factor is $SF_{eq}=SF/U$. N_g-length of cyclic prefix (CP) insertion is also applied. Note that chip-spaced discrete time representation is used throughout this paper.

2.1. Transmit Signal

As illustrated in Fig. 1(a), most of the processes are done in frequency domain. Each symbol in the uth sequence $\{d_u(0),d_u(1),\ldots,d_u(M-1)\}$ is firstly transformed into frequency domain by M-point discrete Fourier transform (DFT) as $\{D_u(0),D_u(1),\ldots,D_u(M-1)\}$, where

$$D_u(k)=\frac{1}{\sqrt{M}}\sum_{n=0}^{M-1}d_u(n)\exp\left(-j2\pi k\frac{n}{M}\right). \quad (1)$$

Next, orthogonal spreading code $C_u(k)$ is applied with particular SF in frequency domain. The resultant chip sequence $\{S_u(k);k=0\sim N_c-1\}$ is expressed by.

$$S_u(k)=D_u\left(\left\lfloor\frac{k}{SF}\right\rfloor\right)C_u(k \bmod SF). \quad (2)$$

The resultant U chip sequences are added and multiplied by a common frequency-domain scramble sequence $\{C_{src}(k);k=0\sim N_c-1\}$. Frequency-domain signal of total resultant U chip sequences after scrambling $\{S(k);k=0\sim N_c-1\}$ is expressed by

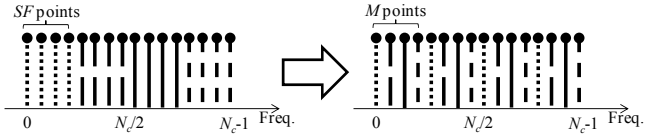

Fig.2 Frequency mapping technique.

$$\begin{aligned} S(k) &= \sum_{u=0}^{U-1}S_u(k)C_{src}(k) \\ &= \sum_{u=0}^{U-1}D_u\left(\left\lfloor\frac{k}{SF}\right\rfloor\right)C_u(k \bmod SF)C_{src}(k) \end{aligned}. \quad (3)$$

We also introduce simple frequency mapping technique as frequency interleaving in order to avoid burst error occurred from severe frequency selectivity. Frequency-domain signal after mapping $\{\widetilde{S}(k);k=0\sim N_c-1\}$ can be expressed by

$$\widetilde{S}(p+q(M))=S(p(SF)+q), \quad (4)$$

where $p=0\sim M-1$ and $q=0\sim SF-1$. Mapping technique can be also illustrated by Fig. 2.

Finally, $\widetilde{S}(k)$ is transformed back into time domain by N_c-point inverse fast Fourier transform (IFFT). Time-domain transmit signal before adding guard interval $\{s(t);t=0\sim N_c-1\}$ after passing through all processes in (1)-(4) is.

$$s(t)=\frac{1}{\sqrt{N_c}}\sum_{k=0}^{N_c-1}\widetilde{S}(k)\exp\left(j2\pi t\frac{k}{N_c}\right). \quad (5)$$

The last N_g chips of each transmission block are copied as cyclic prefix (CP) and inserted into guard interval placed at the beginning of each block and then the signals are transmitted. In summary, we also illustrate the transmission processing of MC-SC-FDSS by Fig. 3.

2.2. Received Signal

The propagation channel is assumed to be a chip-space L-path frequency-selective block fading channel [1], where its impulse response is

$$h(\tau)=\sum_{l=0}^{L-1}h_l\delta(\tau-\tau_l), \quad (6)$$

where h_l and τ_l are complex-valued path gain and time delay of the l-th path, respectively. $\delta(\cdot)$ is the delta function. From (5) and (6), time-domain received signal after CP removal $\{r(t);t=0\sim N_c-1\}$ can be represented as

$$r(t)=\sqrt{\frac{2E_c}{T_c}}\sum_{l=0}^{L-1}h_l s(t-\tau_l)+n(t), \quad (7)$$

where E_c and T_c are chip energy and chip duration, respectively.

N_c-point fast Fourier transform (FFT) is applied to transform $r(t)$ into frequency-domain components $\{R(k);k=0\sim N_c-1\}$. The kth frequency-domain component $R(k)$ is expressed by

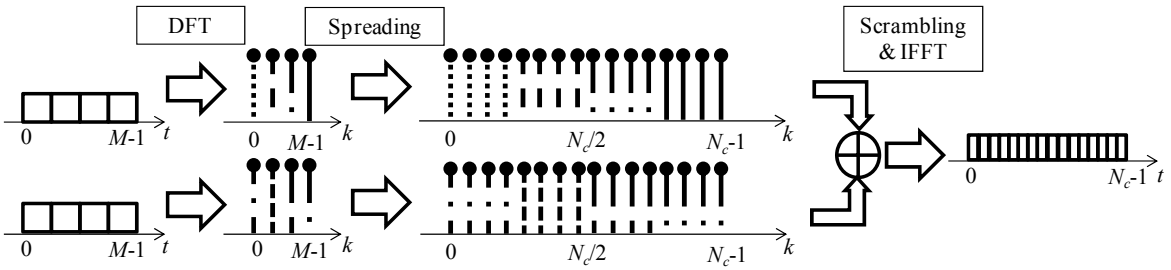

Fig.3 Transmission processing of proposed MC-SC-FDSS.

$$R(k)=\sqrt{\frac{2E_c}{T_c}}H(k)\widetilde{S}(k)+N(k), \tag{8}$$

where

$$\begin{cases} H(k)=\dfrac{1}{\sqrt{L}}\sum_{l=0}^{L-1}h_l\exp\left(-j2\pi k\dfrac{\tau_l}{N_c}\right) \\ N(k)=\dfrac{1}{\sqrt{N_c}}\sum_{t=0}^{N_c-1}n(t)\exp\left(-j2\pi k\dfrac{t}{N_c}\right) \end{cases}. \tag{9}$$

De-mapping is employed on $R(k)$ and $H(k)$ in order to reconstruct the mapping which is employed at the transmitter, yielding $\widetilde{R}(k)$ and $\widetilde{H}(k)$ as

$$\begin{cases} R(p+q(M))=\widetilde{R}(p(SF)+q) \\ H(p+q(M))=\widetilde{H}(p(SF)+q) \end{cases}, \tag{10}$$

where p=0~M-1 and q=0~SF-1.

2.3. Joint FDE and De-spreading

In this subsection, MMSE-FDE and de-spreading are concluded and employed simultaneously. We begin with the frequency-domain received signal of the uth sequence after multiplying the joint FDE and de-spreading weight, which is

$$\begin{aligned} \hat{R}_u(k) &= W_u(k)\widetilde{R}(k) \\ &= \sqrt{\frac{2E_c}{T_c}}\sum_{u'=0}^{U-1}\left\{\widetilde{H}(k)W_u(k)C_{u'}(k)C_{src}(k)D_u\left(\left\lfloor\frac{k}{SF}\right\rfloor\right)\right\}, \\ &\quad + W_u(k)N(k) \end{aligned} \tag{11}$$

where $\{W_u(k);k=0\sim N_c-1\}$ is FDE weight for the uth sequence.

$W_u(k)$ in this paper is derived so as to minimize the mean-square error (MSE) between frequency-domain transmit signal before spreading and frequency-domain received signal after de-spreading. Equalization error of the uth sequence at the kth frequency component $e_u(k)$ is expressed by

$$e_u(k)=\hat{R}_u(k)-D_u\left(\left\lfloor\frac{k}{SF}\right\rfloor\right). \tag{12}$$

By deriving $W_u(k)$ which minimize the $E[|e_u(k)|^2]$, The FDE weight can be expressed by

$$W_u(k)=\frac{\{C_u(k)C_{src}(k)\widetilde{H}(k)\}^*}{\sum_{u'=0}^{U-1}\left|C_{u'}(k)C_{src}(k)\right|^2\left|\widetilde{H}(k)\right|+(\frac{E_c}{N_0})^{-1}}. \tag{13}$$

Note that $|C_u(k)C_{src}(k)|^2$=1 in case that $C_u(k)$ and $C_{src}(k)$ are unit-magnitude.

After applying joint MMSE-FDE weight and de-spreading, frequency components after de-spreading in each stream $\{\hat{D}_u(0),\hat{D}_u(1),...,\hat{D}_u(M-1)\}$ can be expressed by

$$\begin{aligned} \hat{D}_u(k') &= \frac{1}{\sqrt{SF}}\sum_{k=k'SF}^{(k'+1)SF-1}\widetilde{R}(k)W_u(k) \\ &= \frac{1}{\sqrt{SF}}\sum_{k=k'SF}^{(k'+1)SF-1}\sqrt{\frac{2E_c}{T_c}}\sum_{u'=0}^{U-1}\left\{\hat{H}_{u'}(k)D_u\left(\left\lfloor\frac{k'}{}\right\rfloor\right)\right\}. \\ &\quad + \frac{1}{\sqrt{SF}}\sum_{k=k'SF}^{(k'+1)SF-1}W_u(k)N(k) \end{aligned} \tag{14}$$

where $\hat{H}_{u'}(k)=\widetilde{H}(k)W_u(k)C_{u'}(k)C_{src}(k)$. The set of $\hat{D}_u(k')$ is finally transformed back into time-domain signal by M-point inverse DFT (IDFT), obtaining time-domain received symbols $\{\hat{d}_u(0),\hat{d}_u(1),...,\hat{d}_u(M-1)\}$ for the uth sequence, that is

$$\hat{d}_u(n)=\frac{1}{\sqrt{M}}\sum_{k'=0}^{M-1}\hat{D}_u(k')\exp\left(j2\pi n\frac{k'}{M}\right). \tag{15}$$

3. BER Analysis

In this section, conditional SINR and BER analysis is derived for the proposed single-code and multi-code SC-FDSS with joint FDE and de-spreading. We begin the derivation of SINR from the received symbol $\hat{d}_u(n)$

$$\begin{aligned} \hat{d}_u(n) &= \sqrt{\frac{2E_s}{T_c}}\left(\frac{1}{M}\sum_{q=0}^{M-1}\overline{H}_u(q)\right)d_u(n) \\ &\quad + \sqrt{\frac{2E_s}{T_c}}\left(\frac{1}{M}\sum_{q=0}^{M-1}\overline{H}_u(q)\sum_{\substack{\tau=0\\ \tau\neq t}}^{M-1}d_u(\tau)\exp(j2\pi q(\frac{t-\tau}{M})\right). \\ &\quad + \frac{1}{M}\sum_{q=0}^{M-1}\overline{N}(q)\exp(j2\pi q(\frac{n}{M})) \end{aligned} \tag{16}$$

where $\overline{H}_u(q)$ and $\overline{N}(q)$ are expressed as follows.

$$\begin{cases} \overline{H}_u(q)=\dfrac{1}{\sqrt{SF}}\sum_{q'=qSF}^{(q+1)SF-1}\sum_{u'=0}^{U-1}\hat{H}_{u'}(q') \\ \overline{N}(q)=\dfrac{1}{\sqrt{SF}}\sum_{q'=qSF}^{(q+1)SF-1}W_u(q')N(q') \end{cases}. \tag{17}$$

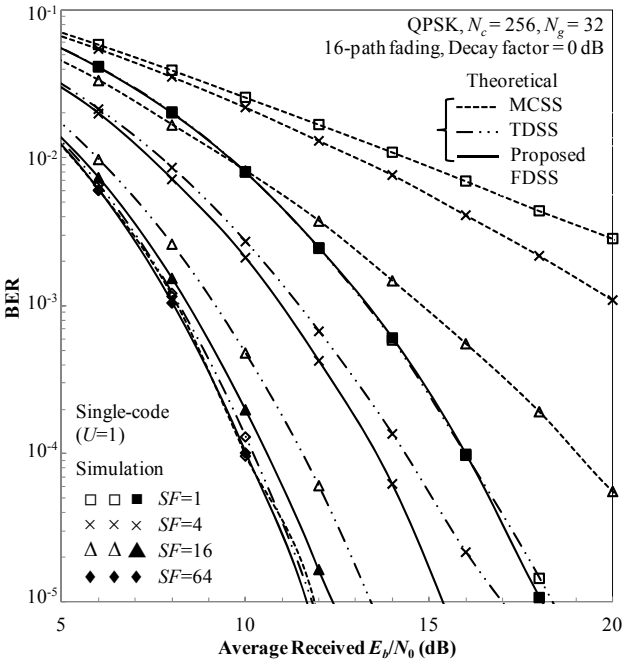

Fig.4 BER performance of single-code transmission.

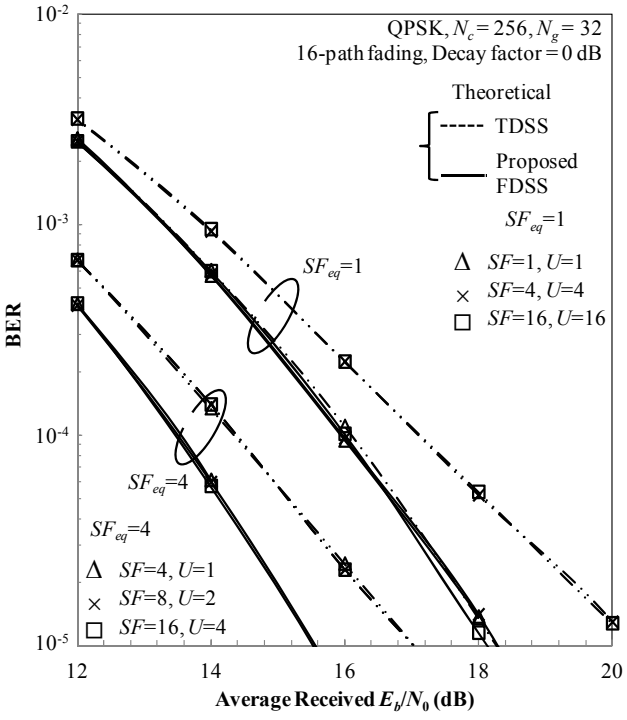

Fig.5 BER performance of single-code and multi-code transmission when SF_{eq}=1 and 4.

From (17), it can be observed that $\overline{H}_u(q)$ is equivalent channel after joint FDE and de-spreading. The second term and the third term in (16) represent residual ISI plus inter-code interference (ICI) in case of multi-code transmission. It can be observed from (16) that $\hat{d}_u(n)$ is a complex-valued random variable with the mean $\sqrt{2E_s/T_s}(1/M)\sum_{q=0}^{M-1}\overline{H}_u(q)d_u(n)$. The variance of interference plus noise $2\sigma_u^2$ can be written as follow.

$$2\sigma_u^2 = \frac{2N_0}{T_s}\left(\frac{1}{M}\frac{1}{SF}\sum_{q=0}^{M-1}\sum_{q'=qSF}^{(q+1)SF-1}\left|W_u(q')\right|^2 + \frac{E_s}{N_0}\left(\frac{1}{M}\sum_{q=0}^{M-1}\left|\overline{H}_u(q)\right|^2 - \left|\frac{1}{M}\sum_{q=0}^{M-1}\overline{H}_u(q)\right|^2\right)\right). \quad (18)$$

Hence, the conditional SINR for given E_s/N_0 and $\{H(k)\}$ is expressed by

$$\gamma_{FD}\left(\frac{E_s}{N_0},\{H(k)\}\right) = \frac{\frac{2E_s}{N_0}\left|\frac{1}{M}\sum_{q=0}^{M-1}\overline{H}_u(q)\right|^2}{\left(\frac{1}{M}\frac{1}{SF}\sum_{q=0}^{M-1}\sum_{q'=qSF}^{(q+1)SF-1}\left|W_u(q')\right|^2 + \frac{E_s}{N_0}\left(\frac{1}{M}\sum_{q=0}^{M-1}\left|\overline{H}_u(q)\right|^2 - \left|\frac{1}{M}\sum_{q=0}^{M-1}\overline{H}_u(q)\right|^2\right)\right)}. \quad (19)$$

In case of single-code transmission, (19) can be simplified as

$$\gamma_{FD,\text{single}}\left(\frac{E_s}{N_0},\{H(k)\}\right) = \frac{\frac{2E_s}{N_0}\left|\frac{1}{M}\sum_{q=0}^{M-1}\widetilde{H}(q)W(q)\right|^2}{\left(\frac{1}{M}\frac{1}{SF}\sum_{q=0}^{M-1}\sum_{q'=qSF}^{(q+1)SF-1}\left|W(q')\right|^2 + \frac{E_s}{N_0}\left(\frac{1}{M}\sum_{q=0}^{M-1}\left[\left|\widetilde{H}(q)W(q)\right|^2 - \left|\frac{1}{M}\sum_{q=0}^{M-1}\widetilde{H}(q)W(q)\right|^2\right]\right)\right)}, \quad (20)$$

which is similar to single-code SC-TDSS.

For simplicity of analysis, the residual ISI, ICI plus noise after FDE is assumed to be zero-mean complex-valued Gaussian random variable [13]. The conditional BER when assuming QPSK modulation is

$$p_b\left(\frac{E_s}{N_0},\{H(k)\}\right) = \frac{1}{2}erfc\left(\sqrt{\frac{1}{4}\gamma\left(\frac{E_s}{N_0},\{H(k)\}\right)}\right), \quad (21)$$

where $erfc(\cdot)$ is complementary error function. The theoretical average BER is numerically computed by averaging (21) over all possible $\{H(k)\}$.

As a comparison, we also consider single-code and multi-code transmissions of TDSS and MCSS [11, 12]. It can be observed that (19), (20), and the SINR in [11, 12] are slightly different, but it is still difficult to exactly determine that which one is the best. To clarify the difference among them, theoretical and simulated BER performance is evaluated in the next section.

4. Performance Evaluation

Numerical and simulation parameters are summarized in Table 1. We assume QPSK block transmission with the number of available subcarriers N_c=256. System performance of both single-code and multi-code

transmissions are evaluated in terms of BER and PAPR, while the BER is also compared with theoretical BER in Section 3.

Table 1 Simulation parameters.

Transmitter	Data modulation	QPSK
	FFT/IFFT block size	N_c = 256
	Code multiplexing order	U=1~16
	Cyclic prefix length	N_g = 32
	Spreading factor	SF=1~64
	Spreading code	Walsh-Hadamard
	Scramble code	Long-PN sequence
Channel	Fading	Frequency-selective block Rayleigh
	Power delay profile	Chip-spaced 16-path uniform
Receiver	FDE	MMSE-FDE, Joint FDE and de-spreading
	Channel estimation	Ideal

4.1. BER Performance

Fig. 4 shows the comparison of BER performances of single-code transmission of proposed SC-FDSS, TDSS, and MCSS as a function of average received bit energy-to-noise power spectrum density ratio $E_b/N_0=0.5(E_s/N_0)(1+N_g/N_c)$. It is seen that the BER performance of proposed SC-FDSS is better than TDSS and MCSS at the same SF. This is because joint FDE and de-spreading minimizes the MSE between the signal before spreading and after de-spreading, indicating that residual ISI is suppressed more in the proposed FDSS, especially when the spreading and de-spreading are done in frequency domain. However, when SF is larger than 16, the BER performance of those transmission schemes are similar since all schemes can achieve the similar amount of diversity gain. It is also noticed that there exist a good agreement between the theoretical and simulated results.

In addition, it is interesting to compare the performance of single-code and multi-code transmissions for the same data rate at the same chip rate (i.e., for the same equivalent spreading factor SF_{eq}). Fig. 5 shows the BER performances of single-code and multi-code transmissions of the proposed SC-FDSS and TDSS at SF_{eq}=1 and 4 (BER performance of MCSS is not included since it is known that its performance is worse than TDSS). It can be seen that the BER of multi-code SC-TDSS is slightly worse when the code multiplexing order U increases at SF_{eq}=1 due to the increase of ICI, where the effect of ICI can be recovered when SF_{eq}=4. However, there is no such effect in the proposed MC-SC-FDSS, implying that joint FDE and spreading can work well even though U is increased.

4.2. PAPR Performance

PAPR over a block transmission is defined as

$$PAPR=\frac{\max\left\{|s(n)|^2\right\}}{E[|s(n)|^2]},\ n=0,\frac{1}{V},\frac{2}{V},...,N_c-1, \tag{22}$$

where V represents oversampling factor. We use complementary cumulative distribution function (CCDF) as an indicator of PAPR performance.

Fig. 6 shows the CCDF of PAPR of the single-code transmissions of TDSS, MCSS, and proposed SC-FDSS when SF=1, 4, and 16. PAPR slightly increases when SF increases in TDSS transmission, where the PAPR at the probability of occurrence of 0.1% (called $PAPR_{0.1\%}$) is about 2.5-3 dB larger than TDSS when $SF\leq4$, and much larger when SF=16 in MCSS transmission. This is confirmed by [14] that PAPR of MCSS with large SF is very large in single-code transmission. On the other hand, the proposed FDSS gives about 1 dB lower PAPR compared to TDSS when SF=4, and then drastically increases when SF=16 due to its interleaving waveform [9].

PAPR of multi-code transmission is also shown in Fig. 7 at SF_{eq}=1 and U=1, 4, and 16, respectively. It can be observed that PAPR of multi-code MCSS remains unchanged when transmit with full multiplexing order [14]. On the other hand, PAPR increases when U increases in both TDSS and proposed FDSS since multiplexing changes the phase rotation of transmit sequence and hence affects the PAPR. However, it is also observed that PAPR of MC-SC-FDSS when SF=4 is still better than TDSS, and becomes closer when SF=16, where it is much larger in single-code transmission. This is because multiplexing reduces the interleaving property of transmit waveform.

5. Conclusion

In this paper, a single-code and multi-code SC-FDSS was introduced, where spreading and de-spreading are done in frequency domain. Joint MMSE-FDE and de-spreading can provide frequency diversity gain and robustness against ICI. Theoretical and simulations results were provided assuming the single-user environment to confirm that the proposed single-code FDSS provides an improvement of BER performance. It was also shown that the PAPR of single-code and multi-code SC-FDSS is better than TDSS when $SF\leq4$, and provides similar PAPR performance in multi-code transmission when SF=16.

References

[1] A. Goldsmith, *Wireless Communications*, Cambridge University Press, 2005.

[2] S. H. Han and J. H. Lee, "An Overview of Peak-to-Average Power ratio Reduction Techniques for Multicarrier Transmission," *IEEE Wireless Commun.*, vol.12, no.2, pp.56-65, Apr. 2005.

[3] H. G. Myung, J. Lim, and D. J. Goodman, "Single Carrier FDMA for Uplink Wireless Transmission", *IEEE Veh. Mag.*, vol.1, pp.30-38, Sept. 2006.

[4] D. Falconer, S. Ariyavisitakul, A. Benyamin-Seeyar, and B. Eidson, "Frequency Domain Equalization for Single-Carrier Broadband Wireless Systems," *IEEE*

Commun. Mag., vol.40, no.4, pp. 58-66, April 2002.

[5] H. Wu, and T. Haustein, "Radio Resource Management for the Multi-User Uplink Using DFT-Precoded OFDM," *in Proc. IEEE International Conf. on Commun. (ICC)*, May 2008

[6] K. Takeda and F. Adachi, "Joint Iterative Transmit/Receive FDE&FDIC for Single-Carrier Block Transmissions," *IEICE Trans. Commun.*, vol. E94-B, no. 5, pp. 1396-1404, May 2011.

[7] A. Boonkajay, T. Obara, T. Yamamoto, and F. Adachi, "Generalized Frequency-Domain Filtered Single-Carrier Transmission", *IEICE Technical Report,* RCS2012-320, pp.219-224, March 2013.

[8] A. Boonkajay, T. Obara, T. Yamamoto, and F. Adachi, "Frequency-Domain Single-Carrier Spread Spectrum with Joint FDE and Spectrum Combining," *to be presented at International Conf. on Information, Commun. and Signal Processing (ICICS 2013)*, December 2013.

[9] A. Boonkajay, K. Adachi, S. Sun, and F. Adachi, "Energy Efficiency of Spread Spectrum Single-Carrier Transmission", *IEICE Technical Report,* RCS2013-75, pp.219-223, June 2013.

[10] J. Joung, C. K. Ho, and S. Sun, "Spectral Efficiency and Energy Efficiency of OFDM Systems: Impact of Power Amplifiers and Countermeasures," to be published in *IEEE J. Sel. Areas. Commun.*, 2013.

[11] K. Takeda and F. Adachi, "Performance Evaluation of Multi-Rate DS-CDMA Using Frequency-Domain Equalization in a Frequency-Selective Fading Channel," *IEICE Trans. Commun.*, vol.E88-B, no.3, March 2005.

[12] F. Adachi, D. Garg, S. Takaoka, and K. Takeda, "Broadband CDMA Techniques," *IEEE Wireless Commun. Mag.*,vol.12, no.2, pp.8-18, April 2005.

[13] T. Yamamoto, K. Takeda, and F. Adachi, "Joint Frequency-Domain Equalization and Despreading for Multi-Code DS-CDMA using Cyclic Delay Transmit Diversity," *IEICE Trans. Commun.,* vol.E92-B, no.5, May 2009.

[14] E. Alsusa and Lin Yang, "MC-CDMA Specific PAPR Reduction Technique Utilising Spreading Code Redistribution," *in Proc. IEEE Veh. Technol. Conf.* (*VTC*) *2006-Fall*, September 2006.

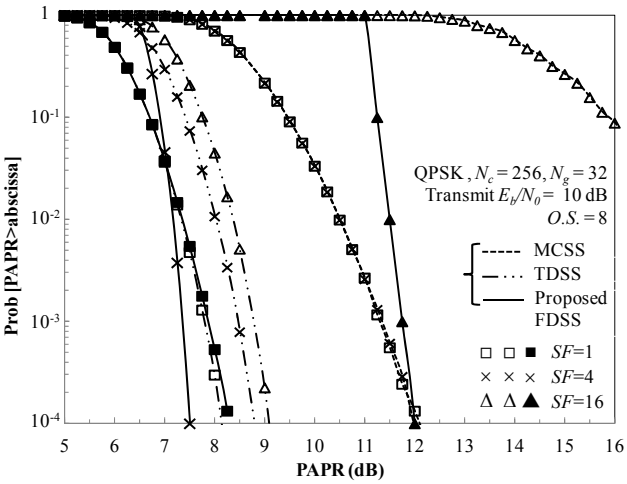

Fig.6 PAPR performance of single-code transmission.

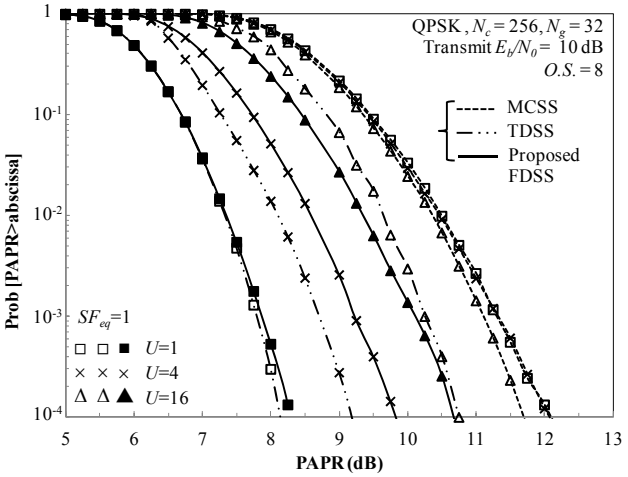

Fig.7 PAPR performance of single-code and multi-code transmission when SF_{eq}=1.